Chapter 8
Operation and Control of a Population of Active Buildings at Network Level

Ben Wooding, Vahid Vahidinasab, Sadegh Soudjani

8.1 Introduction to Control of Active Building Energy Systems

Buildings are seen traditionally as passive loads in the power system. Their users consume electricity, gas and water and pay for these services via some predefined tariffs. The recent evolution in smart devices and the integration of *distributed energy resources* (DERs) and storage systems enables buildings to transition toward a responsive player in the energy systems. Such buildings are called *Active Buildings*.

The future of active buildings is complex. Buildings are smarter and they are coupled to complex components, known as DERs. Buildings can generate their own energy using *photovoltaic panels* (PVs) and store that energy in *energy storage systems* (ESSs) to consume later. An active building can charge an EV it is connected to and manage building temperature through TCLs. Building management systems are able to control these DERs to optimise the building's energy efficiency, even becoming self-sufficient from the power grid.

As the demand-side of the power grid contains more DERs, it also becomes smarter. The *smart grid*, is able to control its frequency and voltage using *demand-side response* (DSR) services from DERs. In this way active buildings become *prosumers*, no longer purely consuming energy from the smart grid but also generating power and injecting it into the grid when necessary or sharing it with local neighbours. Chapter 7 of this book, titled "Control and Management of Active Buildings", discusses coordination structures and control methods for active buildings. In

Ben Wooding
School of Computing, Newcastle University, 1 Science Square, Newcastle upon Tyne, United Kingdom, NE4 5TG e-mail: b.wooding1@newcastle.ac.uk

Vahid Vahidinasab
Department of Engineering, School of Science and Technology, Nottingham Trent University, Nottingham, United Kingdom, NG11 8NS e-mail: vahid.vahidinasab@ntu.ac.uk

Sadegh Soudjani
School of Computing, Newcastle University, 1 Science Square, Newcastle upon Tyne, United Kingdom, NE4 5TG e-mail: sadegh.soudjani@newcastle.ac.uk

this chapter, a detailed discussion of how active buildings can implement smart grid control schemes (e.g. aggregation, multi-vector control and cyber security concerns) to provide services is presented. These services include frequency response and voltage support services.

A detailed case study is also provided, the study considers a population of active buildings which are coupled to TCLs and ESSs. These devices are used to provide energy for frequency services. *Formal control synthesis* and *model predictive control* (MPC) are used to determine the optimal control strategy for the devices. These techniques are then combined for a multi-vector control method.

8.2 Control of a Population of Buildings

8.2.1 Aggregate Models for a Population of Buildings

To manage energy production and consumption and to increase stability of the network, *aggregators* and *demand-side management* (DSM) are suggested for DSR. DSR is demand-side balancing of the generation and consumption of the power network. This is a smart grids most important function. It is vital that energy resources are carefully managed and controlled.

Currently difficulties are present with the supply-demand balance. If the consumption increases above a predicted peak value, then generation companies have to increase their energy production, or if the user consumption of energy is lower than predicted, then resources may be left unused. In both scenarios the operator will experience unnecessary additional costs, and potentially wasted resources [1].

Demand response can occur at a speed almost real-time, and can produces stabler systems with significantly reduced generation costs. In residential sectors, operators take most of the demand response benefits for themselves. Each building in a city or district level network has negligible negotiating power with the operators in the energy market. On top of this, the number of homes in a residential area contributes to scalability challenges and the operator is unlikely to manage negotiations of this scale. This combination; minimal negotiating power combined with high numbers of buildings, poses a challenge to demand response schemes [2]. A viable solution that has been developed is that of the aggregator.

The aggregator works as a middleman, between the operator and individual buildings in the residential region, see Fig. 8.1. The aggregator represents a group of buildings of end-users. At the energy market, the aggregator negotiates on their behalf. Since the aggregator represents a sizeable amount of demand, it is able to negotiate more effectively with the operator. This mainly happens with industrial buildings but is being transitioned into the residential sector as well.

The aggregator pays a fee to end-users to gain control over that buildings appliances. By controlling the appliances of the buildings, the aggregator is able to respond to peak-demand emergencies. It can turn appliances off which are using

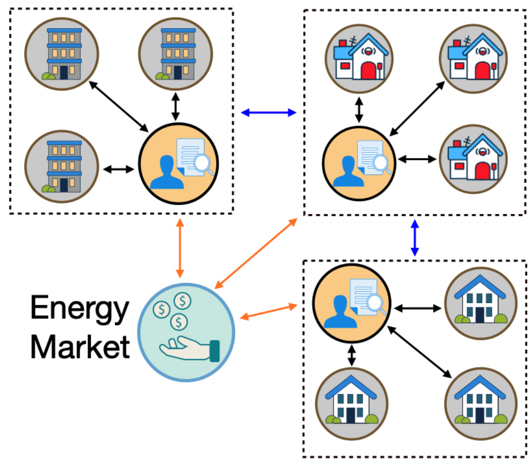

Fig. 8.1: The aggregator is able to negotiate on behalf of the end-users it represents with the energy market and with other aggregators.

sizeable amounts of energy, such as air conditioning units. This reduces the demand side load and returns stability to the network.

By using an aggregator, individual buildings are also able to reduce their energy costs. The aggregator is aware of the total demand profile of the buildings it represents, and pays them incentives to adjust their demand pattern. By scheduling loads to lower cost time periods, the operator is also able to save money on energy resources. The operator rewards the aggregator for it's work in this service. By using this technique, both the aggregator and the end-users can have noteworthy financial benefits, despite the dominant position of the utility operator.

Demand response also has applications for EV charging schemes [3]. The aggregator can schedule when an EV charges, so as to reduce its load on the network. From a high level perspective, the aggregator allows for collections of power units to be treated as a single power unit. This is because the aggregator manages the details of demand response within that group. By using an aggregator, it is possible to simplify and scale many models which include smart buildings, EVs, and other power units.

8.2.2 Frequency Control and System Inertia

Frequency instability is the inability of the power system to maintain a global frequency value after a disturbance occurs which triggers rotor speed changes in the generators. The frequency may rise or fall out of the given operational range. Usually instability is caused by an imbalance between the active power generation and the loads present in the system. Poor coordination, poor protective equipment, slow response times and lack of generation reserves are all possible reasons why instability would occur after a disturbance [4].

One of the control techniques to face the load and generation imbalance is *peak load shifting*. Over a 24 hour period, different hours of the day experience different load values. For example, during the day the system load is highest because people are awake and working. Large machines are also in operation which require large sums of power. At night, the opposite would be the case, people are asleep and machines are turned off. Load shifting attempts to move some of the demand from peak hours to off-peak hours, such as EVs which could charge overnight when their owners would be sleeping. By rescheduling the load away from peak hours, the amount of active power generation required at peak times decreases, providing multiple economic, environmental and efficiency benefits [5].

As the number of EVs connected to the electricity grid is expected to increase. A large load will be present within the system. In [6], residential homes with EVs are used to reduce the expected power system load of higher EV penetrations. A smart charging method is proposed which utilises aggregators to schedule the EV charging times. Using a method similar to MPC, the process is able to update, depending on user travel requirements and conditions of the power system. By reducing annual peak loads, the algorithm is able to reduce the charging costs for the EV owners and also defer system upgrades that would be required for the system with increased load.

Another important consideration is the *rate of change of frequency* (RoCoF). RoCoF is inversely proportional to the available inertia in the power system. When there is low inertia, RoCoF is high which means that system is more volatile and large disturbances could destabilise the system, causing load shedding [7].

Renewable energy sources like PVs do not provide any inertia to the system [8]. This is unlike the large synchronous generators which have kinetic energy stored in their rotated mass that can be released. Therefore, with a global desire to decarbonise the energy systems and accelerate the transition to renewable based energy systems, RoCoF will increase unless managed.

One developing solution is virtual synchronous generators (VSGs), which provides the grid with a variable virtual inertia. The VSGs consist of short-term storage with an inverter and an efficient control mechanism. The VSG reproduces the dynamic properties of real synchronous generators and keep the advantages they provided which include adjusting active and reactive power [9].

Fixed speed wind turbines use an induction wind turbine to provide inertia response for frequency deviations, although the inertia provided is small compared to the inertia of a synchronous generator. For variable speed wind turbines, permanent magnet synchronous generators are used to provide power to the grid, but these are decoupled and so do not provide any frequency response services as well as not storing any reserve power. Techniques are developing that can release the kinetic energy stored in the rotating blades within 10 seconds to help with frequency response, this is known as *inertia emulation* and uses a *fast power reserve* [7].

For PVs, a deloading technique is used which increases the PV voltage beyond the maximum power point (MPP) voltage and allows the PV to retain some reserve power [10]. When the system frequency deviates, this reserve power can be released. However, all PVs will release the same value of power into the grid, and those with less reserves will reach MPP faster and stop contributing to the frequency response, this may cause a second frequency drop once the reserve power is used up.

Another technique to support renewable sources for frequency response is ESS devices, the ESS provides active power to try and prevent a second frequency drop in the system, but also acts as a backup system to provide power if there are any deficits. Coupling ESS with wind or solar can help alleviate the risks of high RoCoF [7, 11].

In [12], it is shown that for low inertia systems, that inertia has little effect on the frequency probability distribution function for small disturbances. So, virtual inertia is insufficient on its own to keep the frequency near the nominal value. Instead, it was shown that the aggregate droop and deadband are the only parameters that have a major influence over the average frequency deviations, which suggests that energy storage solutions are viable and valuable for future smart grid frequency response services.

8.2.3 Coordinated Volt/Var Control

With the increase in renewable penetration in *transmission network*, and increased DERs in the *distribution network*, voltage control is facing significant challenges. On top of this transmission network and distribution network are increasingly coupled, meaning both sides need to effectively be coordinated for the voltage control of the both networks. All these challenges require a greater understanding of the problem and developing advanced control techniques.

Three main control techniques exist. Restoring and maintain the system within a safe working region is known as *corrective control*. *Coordinated control* tracks a set value and mitigates disturbances. *Preventative control* tries to fix the system before any instability occurs and may use fast-response dynamic reactive power (DRP) to facilitate this. Choosing the correct control scheme may depend on response times, control cost and control effectiveness [13].

Transmission Network

Voltage control on the transmission network has been successful for a long time, however the power network is evolving with more renewable resources being incorporated. High penetrations of wind or solar generation have a high risk of causing voltage fluctuations. The use of HVDC lines to connect onshore and offshore wind farms to the transmission network also has the potential for cascading failures, an example cause is DC-blocking contingency. When the fault occurs, in $2-3$ seconds the voltage will increase significantly. This may lead to curtailment of the renewable sources. For this reason, preventative control methods should be applied to wind and solar plants using DRPs for fast-response. HVDC lines have some fast-response reactive power regulation capabilities and so can also support this control scheme [14, 15].

Short-term voltage-instability is usually linked to induction motor stalling and are also known as *Fault Induced Delayed Voltage Recovery* (FIDVR) issues [16]. To mitigate FIDVR, dynamic reactive power sources such as *static reactive power compensators* (SVCs), *static synchronous compensators* (STATCOMs) and DERs are used. The control challenge is the optimal sizing and placement of these sources. Both aspects require the computation of the post-fault voltage trajectory which requires solving differential algebraic equations. These equations are complex due to the nonlinearity of the input-state behaviour and of the solution space, which is also nonconvex. For solving the optimal placement, selection of contingencies must be considered. Depending on the number of reactive power sources, these factors can cause a heavy computational burden. Usually solutions are found using *mixed integer programming* and *heuristic optimisation* algorithms.

For long-term voltage instability detection, the Thévenin equivalent is one method used to present a model of power supply with a fixed impedance to a voltage source for analysis. When the load impedance magnitude equals the Thévenin equivalent impedance then the maximum power supply occurs. This is known as the impedance matching principle and from it the voltage stability margin can be computed. When using measurement data there are challenges from load variations and measurement noise. SCADA and *phasor measurment unit* (PMU) data are used for these computations. There are three methods which are valuable for both online and offline estimation. These are; 1) using the least mean squares to fit the data to the power-voltage curve of the Thévenin equivalent, 2) using data and a real-time algorithm to estimate the Thévenin equivalent from a given bus, 3) estimation of Thévenin reactance to compute the Thévenin voltage. Verifying and validating these measurement based approaches is a future research area [17].

Distribution Network

The increased penetration of DERs, has lead to stricter grid connection requirements. The interconnection of these devices has changed the grid loading pattern and influences voltage regulation device performance. In particular there are four challenges that high DER penetration has caused for voltage regulation in the distribution network.

Firstly, the *distribution system operator* (DSO) has to manage voltage rise. This is often triggered by the generation of solar energy from residential PVs [18]. The injection of too much power into the grid triggers a voltage rise in the system and to mitigate the problem the operator may impose conservative limits on PV installation. A solution is for the PV to self-regulate its voltage by reducing its active power injection or applying negative reactive power injection. Coordinating the PV inverters with demand-side management is another solution. Heat pumps, EVs, or battery storage could be coupled to the PV to increase their consumption of energy to match the PV generation injected.

Secondly, the increase in EVs in the power system could lead to overloads and large voltage drops, especially at peak times. Charging a single EV demands nearly the same energy as three houses. China, India, France and the UK have promised to phase out gas and diesel vehicles by 2040, so, with more vehicles becoming electric the load on the grid is going to increase and control methods such as load shifting and charging strategies will be necessary to avoid overloading the system [6]. Similar to the solution for voltage rise, demand-side devices can support the network to return the voltage to its nominal value. Collections of these devices can form ‘support groups’ around different network buses in the system. A case study using this technique for control of the IEEE 24-bus reliability test system (RTS) is given in [13]. When low voltage buses are discovered in the system the support group would be tasked with returning the system voltage to its expected region.

Thirdly, the distribution network is designed for unidirectional power flow. *Line voltage regulators* (LVRs) are included in the network for voltage control from the load side. If a DER increases the voltage where it is situated, the LVR will try to reduce this from a load side. However, it is possible the voltage at the DER connection point would remain high. Even if the LVR could participate in bidirectional power flow, the DER and/or local voltage correction devices would be needed to stabilise the network. In [19], reactive power control options are coordinated to avoid the continuous operation of devices such as LVR. This avoids both device deterioration and operation of devices at their control limit.

Finally, cloud cover variations affect PVs and can lead to voltage fluctuations and lower power quality across the distribution network. Higher deadband and slope values would ensure system stability of the volt-var curves, but also lead to a reduced range of the voltage margin. Other solutions, such as coupling the DERs for coordinated control could be successful [20].

Transmission/Distributed System Operator Coordination

For voltage control it is also necessary to coordinate the control of the *transmission system operator* (TSO) and the DSO. This is to prevent reactive power exchange when the reactive power is low in the transmission network. A distribution network with coordinated DERs can flexibly adjust its reactive power consumption to provide power reserves and improve the transmission network voltage. There are two types of coordination of the TSO and DSO, these are rule-based methods and distributed optimisation. Both methods involved exchanging boundary voltage and power with one another to stabilise both the transmission network and the distribution network. The distribution network can help by providing fast-response power injection into the transmission network or by reducing their demands and increasing local generation. If the distribution network control scheme ignores the transmission network conditions, it is possible long-term instability will result. To analyse the transmission-distribution reactive power support, a co-simulation of the transmission-distribution is needed.

Effective coupling of the transmission networks and distribution networks leads to economic benefits, as a transmission network does not need to invest in voltage control devices, and can leverage the DERs of the distribution networks [17].

8.2.4 Coordinated Control of Buildings as a Multi-vector Nano Energy Hub

Since the buildings are a junction for the interconnection of multiple energy vectors including electricity, gas, water, renewable energy resources, and transportation, they should be modeled and studied as a multi-vector nano energy hub. This is the reason that buildings will play an important role in the energy context. Considering the increasing global awareness about the holistic approach to energy issues [21], control and operation of the buildings of the future need to be revised in such a way that they can be efficiently managed and controlled, this will accelerate the transition to decarbonisation. Due to the different dynamics and specifications in each energy vector, control of integrated coupled energy systems inside a building is a tough task.

District energy systems attempt to manage and control multiple vectors, this makes them complicated, they require a detailed understanding of both modelling and optimisation. Multi-vector control is the requirement to control modern energy networks that consist of coupled vectors. Previously, heat, electricity, water and gas have been controlled independently but this is no longer suitable for the future smart grid. For example, a heat pump may use electricity to create heat or a combined heat and power unit (CHP) creates electricity from heat and gas. Controlling just a single vector may actually provide lesser control strategies than the combined approach. In one example, a framework is developed that assesses technical, economic and environmental (TEE) benefits of integrating gas and electricity distributed networks with storage devices and discussed how a vector coupling storage system is able to increase whole energy systems efficiency [22].

Understanding the multi-vector components provides increased accuracy in the control. Solar and wind energy are both very uncertain. Solar energy generation uncertainty comes from its proportionality to solar irradiance, but wind speed is the hardest energy source for modelling and prediction. When accurately modelled, a component such as CHP, which uses a heat byproduct from the electricity generation of natural gas, can increase its energy efficiency. In the case of CHP, this can be an increase from $30-40\%$ to $80-90\%$ [23].

Power-to-gas (P2G) is an interesting developing technology. It is used to store excess electricity from stochastic renewable power as either hydrogen or methane gas when it cannot be utilised. These gases can then be used in other areas such as fuel for hydrogen vehicles or by injection into the gas network. P2G is still largely being tested, and there is some worry about high costs and a low conversion efficiency. But a major benefit of this technology will be the large amounts of wind energy storage it can provide.

Buildings also require modelling as they will be integral to future smart grids and district energy systems. The buildings are prosumers and take part in demand side control.

- **White box model** - based on the physical principles of the building;
- **Black box model** - based solely on data;
- **Grey box model** - hybrid approach of white and grey box modelling.

Grey box models and black box models are effective for modelling many building variables. But white box models of buildings are less effective, this is particularly for the cases of real-time optimisation with time-steps less than an hour.

In [24], an Integrated Whole Energy System (IWES) model is used to quantify the benefits of using a multi-vector approach with regards to active buildings. Using a whole system modelling approach shows significant economic saving opportunities. The combined flexibility can increase the proportion of electricity production from renewables and reduce the reliance on low carbon generation like nuclear power. This flexibility will also work for decarbonisation and reaching carbon emission targets. As efficiency of the active building improves the total system costs reduce. Modelling active buildings as multi-vector systems allows for system complementing behaviours to be recognised. An example of this in an active building could be *thermal energy storage* (TES) which would charge thermal energy when the carbon intensity of electric heating is low and discharge it when it is high. These can improve short-term operational costs as well as long-term investment costs as well as reducing carbon emissions. In the report, cost savings were doubled when considering a multi-vector approach.

8.2.5 Security Aspects of Coordinated Control of Active Buildings as a Cyber-Physical System

From a high level power system perspective, the major danger of a cyber attack is if it can permeate through the network. Localised instability, or failure, should be prevented from affecting other areas of the network. Should this mitigation fail, it might trigger cascading failures across the whole network, which would have certain economic consequences as well as possible consequences to transportation (e.g. airports), healthcare (e.g. hospitals), and/or education (e.g. universities/schools).

Sensors and actuators are critical resources for power system control. These devices may connect to an Internet of Things (IoT). Devices of the IoT are known to have vulnerabilities, either on the device directly or through applications that connect to them e.g. a linked smartphone app. One example attack could be the *Manipulation of Demand via IoT* (MadIoT) attack. An attack intending to deliberately cause load shedding in the system, which would have huge repercussions. In [25], a discussion is given about how the attack could be resisted. The solution describes embedding protections into the operation of the transmission grid. Another proposed solution, from [26], regards deterministic virtual networks (DVNs) - a lightweight encryption which would provides security, privacy, performance and energy efficiency to the IoT.

In 2017, a cyber security researcher proposed a cyber attack known as the Horus scenario which targets PV panel inverters. Consider thousands of PV panels on the rooftops of European residential buildings, an attacker might send a signal which would be picked up by these PV panels, and cause them to stop storing energy. The aggregate loss of energy across the power network would then lead to load shedding schemes across the continent.

In a response from SMA Solar Technology, the low likelihood of this attack was shown. Three factors are given that show cyber attacks of this kind require significantly large efforts when attempting to destabilise the grid network. They are; distributed regenerative power generation, decentralized production and the heterogeneity of the PV devices and manufacturers. In essence, it was said that diversity in the grid was the important feature for its safety. An attack would need to simultaneously affect multiple distinct types of devices. Even the large-scale use of bots would have limited success as each system would require an individually configured attack profile [27].

Ultimately, the danger of any cyber attack in the smart grid is related to its communication channels. As a smart grid relies on sending information, communication specific security requirements need to be evaluated. From known security standards, the key parameters that relate to communication are as follows:

- **Confidentiality** - only those with permission should be able to read communicated information;
- **Authentication** - the true sender should be known to the receiver of the communication;
- **Integrity** - information should arrive as it was sent, without any tampering;
- **Access Control** - access to the communication network should only be available to those with the correct clearance;
- **Non-repudiation** - a sender or receiver should not be able to deny their part in a transaction;
- **Availability** - communication channels should not fail, communication should always be possible.

An attacker would benefit should they exploit any one of these principles. Providing authentication and integrity are particularly applicable to a distributed network. Distributed network nodes are fluid and may connect and disconnect from the network at any time (e.g. EV that disconnects to drive). Sender-receiver pairs are unpredictable and depend on the current network state, as well as which nodes are active. Exploiting these could lead to man-in-the-middle attacks, impersonation, message editing or forgery [13]. One defensive authentication technique is digital signatures via hashing and decryption. The receiver compares the senders signature with a known signature of that sender. If the signatures match, the receiver can be confident in the senders authenticity and that the message had not been tampered with.

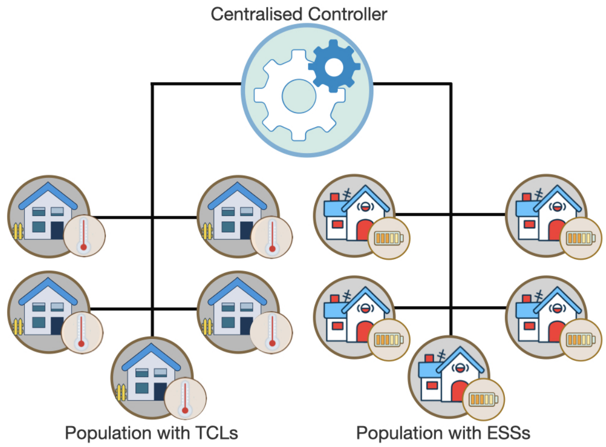

Fig. 8.2: The case study consists of a population of buildings with connected ESSs and TCLs.

Another dangerous cyber attack is the replay attack, which would listen and copy a message as its being broadcast. The attacker then sends this message again, some time in the future, attempting to use it maliciously. If a harmful message is replayed it could cause quite problematic consequences. To address this problem, the receiver needs to know that it has received the message before. Timestamps or random number sequences embedded in the message can provide a good solution.

8.3 Case Studies

In this section, we provide a case study for frequency control. In Fig. 8.2, a population of active buildings is shown. Each building contains either a TCL or an ESS. ESSs and TCLs are combined to provide a demand-side energy response. A centralised controller sends a signal to these buildings to use their respective building components when required. When required the ESSs is able to charge or discharge energy to provide a response service. The TCLs can also provide energy for response services by changing their thermal setpoint, reducing or increasing their consumption of energy from the grid. This case study is broken into four subsections, in the first two subsections we discuss formal control synthesis and use it for frequency control using ESSs. In the third subsection, we use MPC power tracking to control the TCLs to a desired setpoint value. In the final section both of these approaches are combined for a joint ESS and TCL demand-side response for frequency regulation.

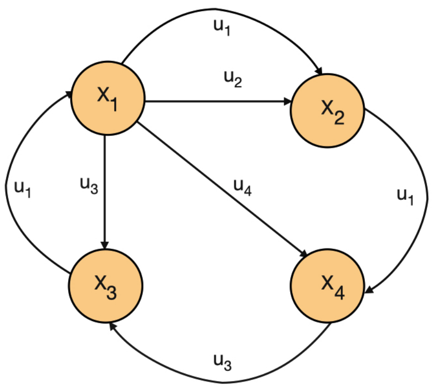

Fig. 8.3: Determinism - for each input u_i applied to a state X_i, a state transition is represented by an arrow. There is at **most** one successor state for each input-state pair.

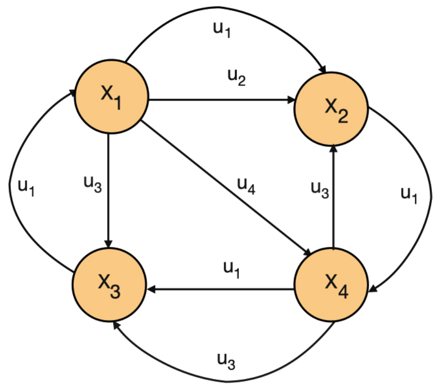

Fig. 8.4: Non-determinism - for each input u_i applied to a state X_i, a state transition is represented by an arrow. There may be two or more successor states for an input-state pair.

8.3.1 Emerging *formal control synthesis* approaches

A system can be described as a mathematical model of a dynamical phenomenon. Different models of the same phenomenon can be used in different tasks, and relationships between those systems can be described [28].

Describing Systems

Infinite-state systems are described by difference or differential equations, depending on whether they are described in discrete or continuous time. The system can be called *deterministic* if for any state x in the system, and for any input u, there is at **most** one successor state. This can be written more formally as in Eq. (8.1).

$$(x \xrightarrow{u} x') \cup (x \xrightarrow{u} x'') \Rightarrow (x' = x''), \forall x, u \rightarrow x \in X, u \in U \tag{8.1}$$

If for an input u at state x, it is possible to have two or more distinct successor states then the system is *non-deterministic*. Different control approaches are needed dependent on the system's determinism. To describe these principles graphically, the most common approach is to use circles for system states with a transition between states represented by an arrow. A notation is added on top of the arrows which shows the input required for the state to undergo the transition. In Fig. 8.3 a deterministic system is shown and Fig. 8.4 shows a non-deterministic system.

Equivalence Property

For infinite-state systems controlling the system's behaviour is difficult. Mostly this is due to the complexity of the system and the computational time and effort required to do any calculations. One tactic is to transform the system to a second, simpler, potentially finite, state system which satisfies the desired *specification* of the system and show it is equivalent to the known infinite-state system, see Eq. 8.2.

$$S_a \cong S_b \tag{8.2}$$

After the transformation, further computations can be completed on this second simpler system. Additionally the system outcomes will be as if they were computed on the more complex system. Even only an approximate equivalence, inside a margin of precision, can provide useful guarantees.

Designing System Specifications

When discussing the equivalence property, it was mentioned that the second system was one that satisfied a desired specification. If a system fails, the economic repercussions will be high. Whether that is purely in lost revenue or repair costs and other aspects affected by a system failure. By designing a rigorous specification that the system holds, it is possible to provide guarantees on system behaviour.

Model checking verifies the system operation against a given specification. The two main specifications for systems relate to safety and reachability. A *safety specification* attempts to control a system within a safe interval while *reachability specifications* check if a system will transition and 'reach' a certain state or set of states. Specifications can also be combined, such as a *reach and stay specification* to reach a safe interval and then remain within it.

Special logic is used to define the system specifications, the two main ones are *Linear Temporal Logic (LTL)* which is used for specifying linear time properties, and *Computational Time Logic (CTL)* used for branching time properties. In this chapter we consider LTL specifications, but further details on both can be found in [29].

Behaviour

Formal control synthesis leverages off the previous discussions on specifications and the equivalence properties. For two systems S_a and S_b, an equivalence is wanted. Consider that S_a relates to an infinite-state system model, and S_b relates to a system which satisfies the desired specification for that system. If the behaviour of S_a is encapsulated inside the system S_b then S_a is behaviourally included in S_b, see Eq. 8.3.

$$B^w(S_a) \subseteq B^w(S_b) \implies S_a \leq S_b \tag{8.3}$$

If both $S_a \leq S_b$ and $S_b \leq S_a$ hold, then the two systems are behaviourally equivalent, acting in the same manner. Extending this notion, it is also proven that under the same actions w, both systems will behave the same, see [28].

$$B(S_a) = B(S_b) \implies B^w(S_a) = B^w(S_b) \tag{8.4}$$

$$B^w(S_a) = B^w(S_b) \implies B(S_a) = B(S_b) \tag{8.5}$$

Formal Control Synthesis

For a system S_a, by finding an equivalent simpler system, S_b, computations for control can be done in less time. The shift to a simpler system is done via an abstraction. The system S_a is partitioned, and each partition is treated as a single *symbolic state* in a *symbolic model*. The symbolic model becomes the equivalent system S_b, and this was shown mathematically in the previous sections.

The desired specification is written in formal language and given along with S_b to a formal methods software tool. The tool attempts to create a formal controller. One guaranteed to satisfy the desired specification for system S_b. If the tool is successful then the new formal controller can be attached to system S_a. As the controller provided guarantees for S_b, it must also provide the same guarantees for S_a, as it is in Eq. 8.4 and Eq. 8.5. Tools used for this type of controller synthesis when the system is under the influence of uncertainty are MASCOT [30, 31], FAUST[2] [32], SReachTools [33], AMYTISS [34], StocHy [35], PRISM [36], among others [37].

8.3.2 Formal control of fast-response elements for frequency regulation

ESSs, such as EVs can connect to the grid through homes or buildings and are used in aggregation for primary frequency response. *Primary frequency response* is the fastest response that the system can provide when a large disturbance event occurs. The ideal scenario returns the frequency to a stable region in as short of a time horizon as possible. In [38], formal control synthesis techniques are used, as discussed in 8.3.1. Formal controller design requires three main steps:

1. **Define the formal specification** - using LTL, the desired system specification is written in a temporal logic. Choosing this specification can be tricky as a good understanding of the system is required in order to define wanted behaviour and unwanted behaviour;
2. **Create the symbolic model** - here the original system dynamics are converted to a symbolic representation by representing partitions of the state space as single symbolic states;

3. **Synthesise symbolic controller** - the symbolic model and the specification are combined to work out legal transitions around the system. Transitions which do not lead to the satisfaction of the specification are removed from the symbolic model. Once this process has finished, any remaining state transitions form the symbolic controller. From the mathematical properties of the system such as bisimulations, the symbolic controller can be applied to the original system with formal guarantees that the specification will be satisfied [28].

To define the formal specification, the GB grid code is used for reference [39]. Two key specifications are determined, these are that the frequency should remain in the safe interval (I_1) of 50 ± 0.5 Hz or for large disturbances only leave the interval for 60 seconds. The frequency should never fall into a containment zone 49.2 Hz. To show the strength of the formal methodology, an additional constraint was added; when the frequency returns to I_1, a second controller should step in and return the system to an even smaller region (I_2). The formal LTL description is shown in Eq. 8.6, where I_1 is the larger safe interval, C_{zone} is the containment zone frequency and I_2 is the smaller safe interval.

$$\begin{aligned}\psi \;:=\; \square(f \geq C_{zone}) \;\wedge\; [\neg(f \in I_1) \implies \lozenge(f \in I_1)] \;\wedge \\ [(f \in I_1 \wedge f \notin I_2) \implies \lozenge(f \in I_2)]\,. \end{aligned} \tag{8.6}$$

To provide a proof of concept, a simulation based on simplified power system dynamics, see Eq. 8.7- 8.9, is used with an expected infrequent infeed loss of 2000 MW. The system is linear and has four dimensions, including the frequency which is the system output. For the system input, the percentage of ESSs which participate in demand-side response is used. Variable values can be found in the original paper [38].

$$\dot{x}(t) = Ax(t) + Bu(t) + B_w w(t), \tag{8.7}$$

$$A = \begin{bmatrix} \frac{-D}{2H} & 0 & 0 & \frac{1}{2H} \\ \frac{1}{T_g R_{eq}} & \frac{-1}{T_g} & 0 & 0 \\ \frac{T_1}{T_2 T_g R_{eq}} & \frac{T_g - T_1}{T_g T_2} & \frac{-1}{T_2} & 0 \\ 0 & 0 & \frac{1}{T_t} & \frac{-1}{T_t} \end{bmatrix} \tag{8.8}$$

$$B = \begin{bmatrix} \frac{p_{av} \times N_{ev}}{2H} \\ 0 \\ 0 \\ 0 \end{bmatrix}, \quad B_w = \begin{bmatrix} \frac{-1}{2H} \\ 0 \\ 0 \\ 0 \end{bmatrix}. \tag{8.9}$$

The formal synthesis is completed inside the SCOTS software tool [40]. Passing the formal specification, system dynamics, maximum and minimum values of the states and size of the partitions into the SCOTS tool will enable it to attempt the formal controller synthesis. As the technique involves removing states from the state space that do not lead to satisfaction of the specification, it is possible for too many transitions to be removed and dead states to exist. In this case the synthesis will have failed and the SCOTS tool returns no controller to the user. From this, a guarantee is given that should the SCOTS tool return a controller to the user then a guarantee is provided that the returned controller will satisfy the specification.

After successfully synthesising the controller for the system, simulations to compare the performance to a baseline controller are devised. The baseline controller accepts the system frequency, Δf, as an input and consists of a frequency deadband, a transfer function and a saturation block to determine the percentage of ESSs required to participate in frequency regulation, Δu. This participation value is multiplied by the aggregate ESS power, P_{ESS}, and number of ESSs, N_{ESS}, to calculate a total demand response from ESSs for frequency regulation at that time instance; as shown in Fig. 8.5.

The control strategy implemented involved several phases which are each represented in the further figures by a shaded colour in the background. In the first phase, there is no initial ESS participation as the frequency is inside the safe interval (I_1), phase shown in light blue. When the frequency leaves the safe interval, the first controller C_1 attempts to return the frequency to I_1 again, phase shown in yellow. Once achieved, controller C_2 takes over and tries to transition the frequency to smaller region I_2, phase shown in white. Upon entering I_2, the ESS participation value is fixed, unless the frequency oscillates outside the region or normal system operation is restored, phase shown in green. In the same manner the baseline controller provides no participation when the frequency is inside the larger safe zone I_1, and this is managed by the deadband.

In Fig. 8.6 and the following figures, the region I_1 is marked in black, I_2 in green, and C_{zone} in red. This model updated every 0.2 seconds. The frequency under the synthesised symbolic controller satisfies the formal specification ψ in (8.6) with $I_1 = [49.55, 50]$ and $I_2 = [49.75, 50]$ Hz, but the baseline controller is unable to shape the frequency with respect to ψ.

To test the robustness of the controller, uncertainty is added to ESS response. Adding a uniformly distributed random uncertainty of up to 10% participation was found to still satisfy the specification as shown in Fig. 8.7, and outperform the equivalent baseline controller. In both controller scenarios the minimum frequency value shifts slightly lower, this is because the uncertainty in the participation reduces

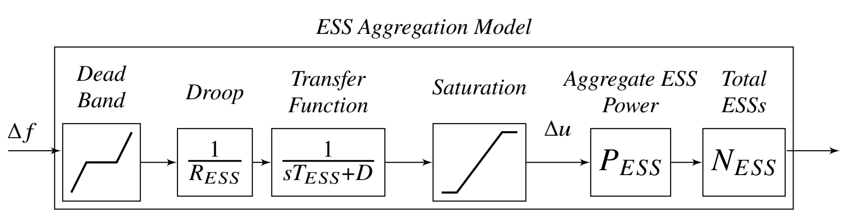

Fig. 8.5: Baseline controller of ESS frequency response services when a large power loss occurs, adapted from [41, 42].

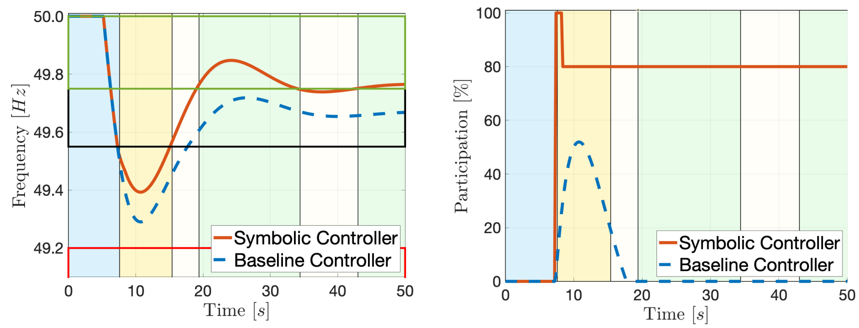

(a) (b)

Fig. 8.6: Symbolic control of the frequency using ESSs **(a)** and the participation of ESSs over time **(b)**.

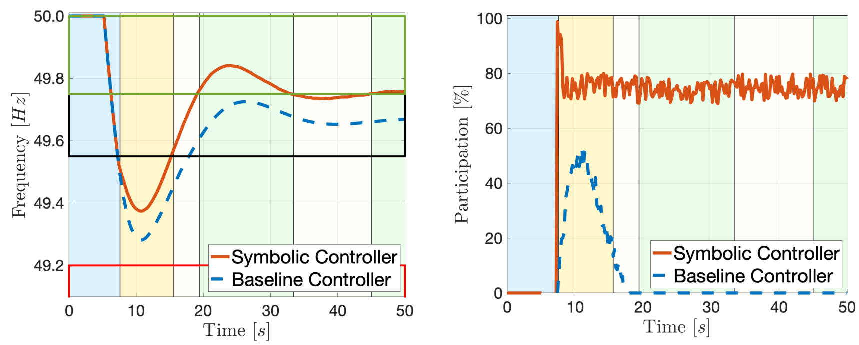

(a) (b)

Fig. 8.7: Symbolic control of the frequency using uncertain ESSs **(a)** and the participation of uncertain ESSs over time **(b)**.

the amount of energy used for response. This leads to a larger RoCoF and so, for the same time horizon, lower frequency values are reached.

This case study approach can also be applied to more complex and nonlinear systems, but with increased computations. Fig. 8.7 showed the results of the system with an uncertain participation value but extensions can also be made to include uncertainty of the plant values or increasing the participation uncertainty. To continue to provide guarantees in the cases of uncertainty, one approach use formal methods for stochastic systems. The guarantees are to a certain confidence level, this can be a % confidence that the guarantees are provided or a full guarantee within a particular range.

8.3.3 MPC-enabled heating/cooling systems for flexibility provision

A component of uncertainty in the power system is renewable generation sources which depend on highly unpredictable factors such as wind speed and solar irradiance. Power tracking is a tool which can be used to control the changes surrounding such uncertainties. TCLs are an example component than can be used for power tracking. By using a temperature setpoint as an input, it is possible to control the energy consumption of the TCLs and use the difference in energy consumption for demand-side response services.

In this section we will discuss a two step formal approach for TCL power tracking using a model based on the probabilistic evolution of the TCL temperature. Firstly, the continuous space model is converted to a finite state model, which obtains a population of Markov chains. Secondly, a cross product of the Markov chain models is done to find the coarsest probabilistically bisimular Markov chain. This abstraction then has guaranteed error bounds. At the end of the section a numerical example will be given; using a modified Kalman filter to estimate the system state space and a one-step MPC for total power consumption.

For the power tracking an accurate TCL model is required. We consider a population of homogeneous TCLs. For a single TCL, the temperature evolution can be given by Eq. 8.10, where θ_a is the ambient temperature, C is thermal capacitance, R is thermal resistance, P_{rate} is the rate of energy transfer, $w(t),\ t \in \mathbb{Z}$ is process noise, and $a = e^{-h/RC}$ with discretisation step h.

$$\theta(t+1) = a\theta(t) + (1-a)(\theta_a \pm m(t)RP_{rate}) + w(t) \tag{8.10}$$

For TCLs which heat, + is used, while for TCLs which cool − is used. $m(t)$ signifies the state of the TCL, if 0 then the TCL is in the OFF state, if 1 then the TCL is in the ON state. The temperature dynamics are regulated by:

$$f(m,\theta) = \begin{cases} 0, & \theta > \theta_s - \dfrac{\delta}{2} \doteq \theta_- \\ 1, & \theta > \theta_s + \dfrac{\delta}{2} \doteq \theta_+ \\ m, & else, \end{cases}$$

where θ_s is the temperature setpoint and δ is the deadband. Together these describe the temperature range. The power consumption of the TCL when in the ON position is given as:

$$P_{rate,ON} = \frac{1}{\eta} P_{rate} \tag{8.11}$$

where η is the *coefficient of performance* (COP). Therefore, the power consumption at time t is:

$$t = m(t) P_{rate,ON} \tag{8.12}$$

From the abstraction given, a single TCL can be considered a *stochastic hybrid system* (SHS). The TCL is a discrete-time Markov process evolving over a hybrid state space characterised by a variable $s = (m, \theta) \in \mathbb{Z}_1 \times \mathbb{R}$. By interpreting the TCL as an SHS, an abstraction technique from [43] can be used to reduce the uncountable state space Markov process to a finite state Markov chain.

We focus on a population of cooling devices but heating devices can be similarly derived. We will represent the homogeneous Markov chain by Ξ. Ξ has the state

$$\mathbf{z} = [z_1, z_2, \ldots, z_{n_p}]^T \in \mathcal{Z} = \mathbb{N}_{2n}^{n_p}, \tag{8.13}$$

where $z_j \in \mathbb{N}_{2n}$ represents the state of the j^{th} Markov chain.

For the second step of the abstraction we wish to further aggregate the model and use a notion of exact probabilistic bisimulation [29]. Given the labelling function, L, an equivalence relation, $\mathcal{R}$, of the state space, $\mathcal{Z}$, is defined such that:

$$\forall(\mathbf{z}, \mathbf{z}') \in \mathcal{R} \Leftrightarrow L(\mathbf{z}) = L(\mathbf{z}') \tag{8.14}$$

The equivalence relation provides a partition of the state space of $\mathcal{Z}$ into equivalent classes belonging to a quotient set $\mathcal{Z}/\mathcal{R}$, where each class is uniquely specified by the label of its elements. A proof is given as to why $\mathcal{R}$ is an exact probabilistic bisimulation relation on Ξ in [44, 45]. From this proof we now have an abstract model of the evolution of the TCL population based on linear stochastic equations. We refer the reader to the papers [46, 47] for closely-related formal treatment of aggregate energy modeling and regulation.

The power consumption of the aggregate model is therefore:

$$y_{total}(t) = \sum_{i=1}^{n_p} m_i(t) P_{rate,ON} \tag{8.15}$$

For the abstract model this is:

$$y_a(t) = H\mathbf{X}(t), \quad H = n_p P_{rate,ON} [0_n, 1_n] \tag{8.16}$$

where the variable $\mathbf{X}$, is the normalised value of the labels $\mathbf{x}$, and $\mathbf{x}(t)$ is a bisimulation of $\mathbf{z}(t)$ of Ξ,

$$\mathbf{z}(t) \rightarrow \mathbf{x}(t)$$

and $[0_n, 1_n]$ are row vectors with all entries equal to 0 and 1 respectively. By finding the difference between the expected values of $y_{total}(t)$ and $y_a(t)$ allows for tuning the error made in estimating the total power consumption of the population from the abstraction.

Finally we will present a numerical simulation of the power tracking. The simulation uses a TCL population size of 500, temperature set point of $20°C$ and a time horizon of 1 hour. Other simulation values can be found in [44].

We set the control input to be the temperature setpoint, θ_s, of the TCL. We apply a control input to all TCLs uniformly, to obtain a homogeneous population of TCLs since this represents no prior knowledge of the state of a single TCL. A prior knowledge of the states in $\mathbf{X}(t)$ is not necessary. Instead, an online measurement of the total power consumption of the TCL population is used which allows estimating

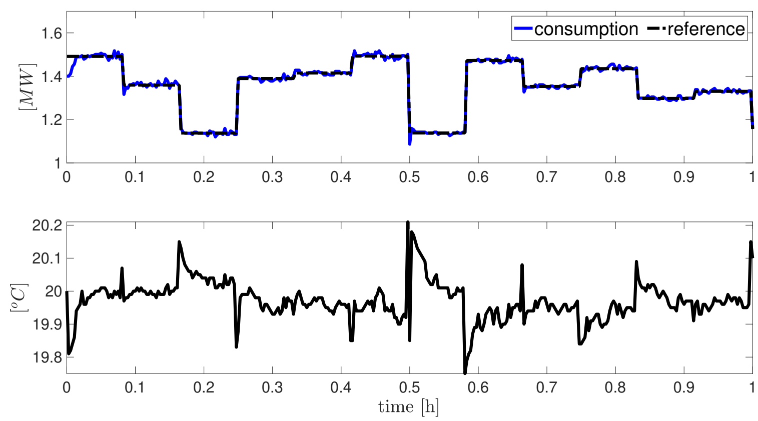

Fig. 8.8: TCL tracking outcome **(top)** and temperature setpoint θ_s **(bottom)**.

the states in **X**(t) and using θ_s to track any reference signal based on a one-step output prediction.

We consider the total power consumption to be:

$$y_m(t) = H\mathbf{X}(t) + v(t) \tag{8.17}$$

where v(t) is measurement noise. The state of the system is then measured using a modified classical Kalman filter. This state estimation is included in a one-step MPC scheme to synthesise the next control input. The obtained optimal value $\theta_s(t+1)$ is applied to the following iteration of the TCL population.

In Fig. 8.8, the outcomes of the TCL tracking of a reference signal is shown for a time horizon of one hour. Here it can be seen that a reference value can be set to control the population of TCLs, when the reference is increased then more power is required and a percentage of TCLs switch to the ON state, when the reference is reduced then a percentage of TCLs switch to the OFF state. From the formal abstraction, we have guarantees over this behaviour and can exactly quantify the error added by the abstraction.

8.3.4 Coordinated control for provision of frequency response services

In the previous two sections, we discussed a formal control approach to provide demand-side response for frequency regulation using ESSs, and power tracking TCLs which were able to accurately follow a reference signal to consume a desired level of energy. In this section we will combine the two approaches to provide a frequency response that consists of both ESSs and TCLs, in a multi-vector control

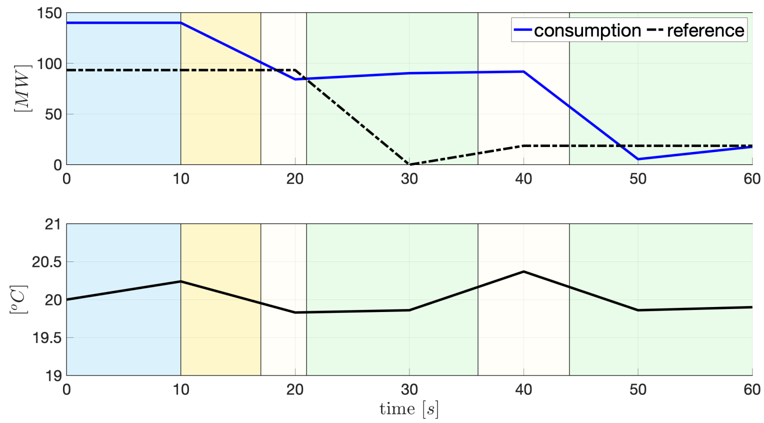

Fig. 8.9: **Top** - TCL reference tracking to provide demand response. **Bottom** - TCL temperature setpoint changes used to track the reference.

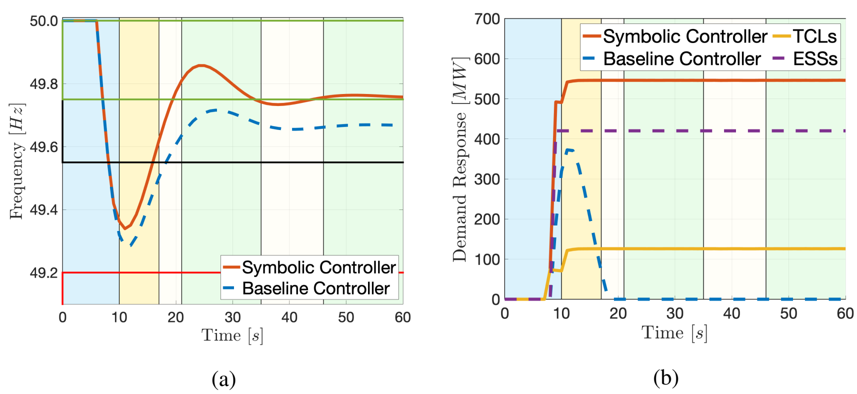

Fig. 8.10: Symbolic control of the frequency using ESSs and TCLs **(a)** and the combined demand response over time **(b)**.

scenario. We decide that the energy used in responding to the frequency loss event will come from both ESSs and TCLs, with a ESS-to-TCL ratio of 3 : 1.

As described in the first section, the symbolic controller chooses a participation value, u_{ESS}, based on the current frequency. Using this participation we can determine the amount of power that the controller is asking to be used for frequency response. By quartering that value, a desired reference, y_{des} is found that can be fed into the power tracking algorithm of the TCLs, see Eq. 8.18 where $N_{ESS} = 25,000$, $N_{TCL} = 50,000$, $P_{ESS} = 0.028$ MW and $P_{TCL} = 0.014$ MW. The desired reference is used to select the setpoint temperature, θ_s, which reduces TCL energy consumption to be used for demand response.

$$y_{des} = (1 - u_{ESS}) \times \frac{N_{ESS} P_{ESS}}{4 N_{TCL} P_{TCL}} \tag{8.18}$$

TCLs respond slower than ESSs as there is a delay for the components to heat or cool to the desired setpoint. This can be seen in Fig. 8.9 where there is a clear delay before the reference value and consumption value align. This consumption value is what will be used in our frequency response model of the TCLs as the delay provides a realistic response of the TCL behaviour. **Note:** the decrease in consumption is equivalent to an increase in energy generation as it will be shown in Fig. 8.10b.

Unlike ESSs, TCLs cannot respond to frequency changes in under a second, so the time-step of the model will be set to 1 second rather than 0.2 seconds as in the previous section.

In Fig. 8.10, it is clear that ESSs and TCLs can combine to perform a valuable frequency response. The performance of the combined approach is slower than for 100% ESS scenario, and the frequency reaches to a lower minimum frequency value than that scenario. However, the combined demand-response still fulfills the requirements given in the formal specification from Eq. 8.6, and provides an improved frequency response compared to the baseline controller. On top of this the slow response requires less initial energy from the responding components than for the purely ESS scenario, where 100% ESSs were asked to participate.

8.4 Status Quo, Challenges and Outlook

To conclude, this chapter has discussed the control and management of a community of active buildings. Specifically, we looked at the control of frequency and voltage and discussed the controls uses in multi-vector energy and aggregators problem, as well as cyber security aspects. Finally, a case study using a symbolic controller for demand-side frequency response of ESSs and TCLs was shown to provide beneficial controls, particularly that the control technique has guarantees on performance.

There are three future directions for researchers to consider having read this chapter.

- Firstly, the smart grid is evolving to be more distributed and electrified as more components join the power network. This increased load will add a strain to the network unless control schemes are developed to safely manage these new components while also keeping users satisfied.
- Secondly, as the smart grid becomes more distributed the need for multi-vector energy controls will keep growing, this requires accurate models of the vector components and also inclusion of distributed resources such as buildings and EVs. The importance of accurate models is a recurring theme of this chapter and will benefit all aspects of control.

- Finally, as more uncertain renewable sources are incorporated into the grid, the amount of system inertia decreases and the RoCoF increases. VSGs and ESSs will become increasingly important to the future of the smart energy systems.

References

1. A. Anees and Y. P. P. Chen, "True real time pricing and combined power scheduling of electric appliances in residential energy management system," *Applied Energy*, vol. 165, pp. 592–600, 2016.
2. L. Gkatzikis, I. Koutsopoulos, and T. Salonidis, "The role of aggregators in smart grid demand response markets," *IEEE Journal on Selected Areas in Communications*, vol. 31, no. 7, pp. 1247–1257, 2013.
3. P. Siano and D. Sarno, "Assessing the benefits of residential demand response in a real time distribution energy market," *Applied Energy*, vol. 161, pp. 533–551, 2016.
4. H. Bevrani, *Robust power system frequency control*. Springer, 2009.
5. P. Devaux and M. M. Farid, "Benefits of PCM underfloor heating with PCM wallboards for space heating in winter," *Applied Energy*, vol. 191, pp. 593–602, 2017.
6. D. Wu, N. Radhakrishnan, and S. Huang, "A hierarchical charging control of plug-in electric vehicles with simple flexibility model," *Applied Energy*, 2019.
7. M. Dreidy, H. Mokhlis, and S. Mekhilef, "Inertia response and frequency control techniques for renewable energy sources: A review," *Renewable and Sustainable Energy Reviews*, vol. 69, pp. 144–155, 2017.
8. Y. Wang, V. Silva, and M. Lopez-Botet-Zulueta, "Impact of high penetration of variable renewable generation on frequency dynamics in the continental europe interconnected system," *IET Renewable Power Generation*, vol. 10, no. 1, pp. 10–16, 2016.
9. H. Bevrani, T. Ise, and Y. Miura, "Virtual synchronous generators: A survey and new perspectives," *International Journal of Electrical Power & Energy Systems*, vol. 54, pp. 244–254, 2014.
10. P. P. Zarina, S. Mishra, and P. C. Sekhar, "Exploring frequency control capability of a PV system in a hybrid PV-rotating machine-without storage system," *International Journal of Electrical Power & Energy Systems*, vol. 60, pp. 258–267, 2014.
11. D. M. Greenwood, K. Y. Lim, C. Patsios, P. F. Lyons, Y. S. Lim, and P. C. Taylor, "Frequency response services designed for energy storage," *Applied Energy*, vol. 203, pp. 115–127, 2017.
12. P. Vorobev, D. M. Greenwood, J. H. Bell, J. W. Bialek, P. C. Taylor, and K. Turitsyn, "Deadbands, Droop, and Inertia Impact on Power System Frequency Distribution," *IEEE Transactions on Power Systems*, vol. 34, no. 4, pp. 3098–3108, 2019.
13. K. M. Rogers, R. Klump, H. Khurana, A. A. Aquino-Lugo, and T. J. Overbye, "An authenticated control framework for distributed voltage support on the smart grid," *IEEE Transactions on Smart Grid*, vol. 1, no. 1, pp. 40–47, 2010.
14. G. J. Kish, M. Ranjram, and P. W. Lehn, "A Modular Multilevel DC/DC Converter With Fault Blocking Capability for HVDC Interconnects," *IEEE Transactions on Power Electronics*, vol. 30, no. 1, pp. 148–162, 2015.
15. M. M. C. Merlin, T. C. Green, P. D. Mitcheson, D. R. Trainer, R. Critchley, W. Crookes, and F. Hassan, "The alternate arm converter: A new hybrid multilevel converter with dc-fault blocking capability," *IEEE Transactions on Power Delivery*, vol. 29, no. 1, pp. 310–317, 2014.
16. M. Paramasivam, A. Salloum, V. Ajjarapu, V. Vittal, N. B. Bhatt, and S. Liu, "Dynamic optimization based reactive power planning to mitigate slow voltage recovery and short term voltage instability," *IEEE Transactions on Power Systems*, vol. 28, no. 4, pp. 3865–3873, 2013.
17. H. Sun, Q. Guo, J. Qi, V. Ajjarapu, R. Bravo, J. Chow, Z. Li, R. Moghe, E. Nasr-Azadani, U. Tamrakar, G. N. Taranto, R. Tonkoski, G. Valverde, Q. Wu, and G. Yang, "Review of Challenges and Research Opportunities for Voltage Control in Smart Grids," *IEEE Transactions on Power Systems*, vol. 34, pp. 2790–2801, 2019.

18. M. Karimi, H. Mokhlis, K. Naidu, S. Uddin, and A. H. A. Bakar, “Photovoltaic penetration issues and impacts in distribution network – A review,” *Renewable and Sustainable Energy Reviews*, vol. 53, pp. 594–605, 2016.
19. Y. P. Agalgaonkar, B. C. Pal, and R. A. Jabr, “Distribution voltage control considering the impact of pv generation on tap changers and autonomous regulators,” *IEEE Transactions on Power Systems*, vol. 29, no. 1, pp. 182–192, 2014.
20. N. Mahmud and A. Zahedi, “Review of control strategies for voltage regulation of the smart distribution network with high penetration of renewable distributed generation,” *Renewable and Sustainable Energy Reviews*, vol. 64, pp. 582–595, 2016.
21. T. Elliott, J. Geske, and R. Green, “White paper: Can you make money from active buildings? challenges facing business models,” Active Buildings Centre Research Programme, Tech. Rep., 2020.
22. S. H. Reza Hosseini, A. Allahham, V. Vahidinasab, S. L. Walker, and P. Taylor, “Techno-economic-environmental evaluation framework for integrated gas and electricity distribution networks considering impact of different storage configurations,” *International Journal of Electrical Power & Energy Systems*, 2021.
23. J. Reynolds, M. W. Ahmad, and Y. Rezgui, “Holistic modelling techniques for the operational optimisation of multi-vector energy systems,” *Energy and Buildings*, vol. 169, pp. 397–416, 2018.
24. G. Strbac, M. Woolf, D. Pudjianto, X. Zhang, S. Walker, and V. Vahidinasab, “White Paper: The Role of Active Buildings in the Transition to a Net Zero Energy System,” Active Buildings Centre Research Programme, Tech. Rep., 2020.
25. B. Huang, A. A. Cardenas, and R. Baldick, “Not everything is dark and gloomy: Power grid protections against IoT demand attacks,” *Proceedings of the 28th USENIX Security Symposium*, pp. 1115–1132, 2019.
26. T. H. Szymanski, “Security and privacy for a green internet of things,” *IT Professional*, vol. 19, no. 5, pp. 34–41, 2017.
27. SMA Solar Technology AG, “Statement by SMA Solar Technology AG on the Cyber Security of PV Inverters (Horus Scenario),” *White Paper*, 2017.
28. P. Tabuada, *Verification and control of hybrid systems: A symbolic approach*. Springer US, 2009.
29. C. Baier and J.-P. Katoen, *Principles of Model Checking*. MIT Press, 2008.
30. R. Majumdar, K. Mallik, and S. Soudjani, “Symbolic controller synthesis for büchi specifications on stochastic systems,” in *Proceedings of the 23rd International Conference on Hybrid Systems: Computation and Control*, ser. HSCC ’20. New York, NY, USA: Association for Computing Machinery, 2020.
31. R. Majumdar, K. Mallik, A.-K. Schmuck, and S. Soudjani, “Symbolic control for stochastic systems via parity games,” *arXiv:2101.00834*, 2021.
32. S. Soudjani, C. Gevaerts, and A. Abate, “FAUST^2: Formal abstractions of uncountable-state stochastic processes,” in *TACAS*, ser. LNCS. Springer, 2015, vol. 9035, pp. 272–286.
33. A. P. Vinod, J. D. Gleason, and M. M. K. Oishi, “SReachTools: A MATLAB Stochastic Reachability Toolbox,” in *Proceedings of the 22nd ACM International Conference on Hybrid Systems: Computation and Control*, ser. HSCC ’19. New York, NY, USA: Association for Computing Machinery, 2019, p. 33–38.
34. A. Lavaei, M. Khaled, S. Soudjani, and M. Zamani, “AMYTISS: Parallelized automated controller synthesis for large-scale stochastic systems,” in *Proc. 32nd International Conference on Computer Aided Verification (CAV)*, ser. LNCS. Springer, 2020.
35. N. Cauchi and A. Abate, “StocHy: automated verification and synthesis of stochastic processes,” in *25th International Conference on Tools and Algorithms for the Construction and Analysis of Systems (TACAS)*, 2019.
36. M. Kwiatkowska, G. Norman, and D. Parker, “PRISM 4.0: Verification of probabilistic real-time systems,” in *Proc. 23rd International Conference on Computer Aided Verification (CAV’11)*, ser. LNCS, G. Gopalakrishnan and S. Qadeer, Eds., vol. 6806. Springer, 2011, pp. 585–591.

37. A. Abate, H. Blom, N. Cauchi, J. Delicaris, A. Hartmanns, M. Khaled, A. Lavaei, C. Pilch, A. Remke, S. Schupp, F. Shmarov, S. Soudjani, A. Vinod, B. Wooding, M. Zamani, and P. Zuliani, "ARCH-COMP20 Category Report: Stochastic Models," in *ARCH20. 7th International Workshop on Applied Verification of Continuous and Hybrid Systems (ARCH20)*. EasyChair, 2020.
38. B. Wooding, V. Vahidinasab, and S. Soudjani, "Formal Controller Synthesis for Frequency Regulation Utilising Electric Vehicles," in *2020 International Conference on Smart Energy Systems and Technologies (SEST)*, 2020, pp. 1–6.
39. National Grid, "The Grid Code," National Grid, Tech. Rep., 2020.
40. M. Rungger and M. Zamani, "SCOTS: A tool for the synthesis of symbolic controllers," in *Hybrid Systems: Computation and Control (HSCC)*. ACM, 2016.
41. C. Mu, W. Liu, and W. Xu, "Hierarchically adaptive frequency control for an ev-integrated smart grid with renewable energy," *IEEE Transactions on Industrial Informatics*, vol. 14, no. 9, pp. 4254–4263, 2018.
42. S. Izadkhast, P. Garcia-Gonzalez, and P. Frías, "An aggregate model of plug-in electric vehicles for primary frequency control," *IEEE Transactions on Power Systems*, vol. 30, no. 3, pp. 1475–1482, 2015.
43. A. Abate, J.-P. Katoen, J. Lygeros, and M. Prandini, "Approximate Model Checking of Stochastic Hybrid Systems," *European Journal of Control*, vol. 16, no. 6, pp. 624–641, 2010.
44. S. Soudjani and A. Abate, "Aggregation and Control of Populations of Thermostatically Controlled Loads by Formal Abstractions," *IEEE Transactions on Control Systems Technology*, vol. 23, no. 3, pp. 975–990, 2015.
45. Soudjani, Sadegh and Abate, A, "Aggregation of thermostatically controlled loads by formal abstractions," in *European Control Conference*, Zurich, Switzerland, July 2013, pp. 4232–4237.
46. M. Kamgarpour, C. Ellen, S. Soudjani, S. Gerwinn, J. Mathieu, N. Mullner, A. Abate, D. Callaway, M. Fränzle, and J. Lygeros, "Modeling options for demand side participation of thermostatically controlled loads," in *International Conference on Bulk Power System Dynamics and Control (IREP)*, August 2013, pp. 1–15.
47. S. Soudjani, S. Gerwinn, C. Ellen, M. Fränzle, and A. Abate, "Formal synthesis and validation of inhomogeneous thermostatically controlled loads," in *International Conference on Quantitative Evaluation of Systems*. Springer, 2014, pp. 57–73.